



## Disintegrations and its Noval Perspectives

*O. Kalyan<sup>1\*</sup>, G. Snehalatha<sup>2</sup>, M. Tulsi<sup>3</sup>, K. Rohitha<sup>4</sup>*

A.U College of Pharmaceutical Sciences Andhra University, Visakhapatnam 530003, Andhra Pradesh, India

E-mail: , [kalyanoru@gmail.com](mailto:kalyanoru@gmail.com) \*<sup>1</sup>, [snehalatha.g16@gmail.com](mailto:snehalatha.g16@gmail.com)<sup>2</sup>, [mctulasi@gmail.com](mailto:mctulasi@gmail.com)<sup>3</sup> [kandregularohitha07@gmail.com](mailto:kandregularohitha07@gmail.com)<sup>4</sup>

### ABSTRACT:

Disintegration is the disaggregation of the solid dosage form into smaller particles upon contact with biofluids. Disintegration is the critical parameter for tablets and capsule dosage forms; the fate of tablet (or) capsule of immediate (or) controlled release in the human body is primarily influenced by this parameter. In this article, we discussed the new insights on the disintegration screening techniques and their scope for the disintegration testing of the dosage forms. Screening techniques are the new thermal imagining by the thermal imager and modeling evaluation of the pore size during the disintegration of pharmaceutical tablets. In tablet pore size modeling evaluation with simulation model formula and steps to the modeling.

### 1.Introduction:

The formulation development department is well established and emerging with new technologies in dosage form preparation. Although there are many new technologies and new dosage forms on the market, tablet dosage forms have their patient compliance. So, the tablets, as they market sustainability, have to undergo new evaluation tests that can ensure their quality and efficacy. Those can give accurate evaluation results for the tablets. The disintegration test was performed by the disintegration apparatus; disintegration is the disaggregation of the solid dosage form into smaller particles upon contact with biofluids [1] it will calculate the disintegration time, but by the new technique known as thermal imaging, we may predict the amount of the dosage form that was disintegrated, the advantage of thermal imaging that can be used indirectly to estimate mass under certain conditions. The modeling evaluation of pore structure during the tablet provides the pore structural influence on the tablet disintegration. During the modeling, we came to know that the tablet compaction, disintegration model, and pore structure analysis.

**Keywords:** Tablet disintegration, Discrete element modelling, Pore size, Tablet thermal imagining, Tablet screening.

### 2.New insights on the disintegration

#### 2.1. Disintegration screening by the new thermal imagining technique [2]:

The authors Jasbir Singh and et.al. reported that solid dosage forms known as rapidly disintegrating tablets (RDTs) which dissolve quickly due to their rapid disintegration. These tablets have various names, including orally disintegrating tablets (ODTs), and dissolve in seconds when placed in the mouth according to FDA Guidance for Industry (FDA, 2008). The guidelines specify a weight limit of 500mg for the tablets but don't mention any restrictions on their size or dimensions [2].

Their research compared infrared (IR) images and thermal imagers. It explained that IR imagers are sensitive to a specific near-infrared range and need an external light source. In contrast, thermal imagers detect the mid- and far-infrared range, where most warm objects emit radiation. The study also mentioned that the high temporal resolution of FTIR imaging systems is due to their external illumination and broader infrared detection range.

The authors described a cost-effective method for directly analyzing tablet temperature using a thermal imager. This setup boasts a high thermal sensitivity of 0.05 °C and can measure temperatures between -20 °C and +650 °C. Additionally, the research highlighted the simplicity of using this method [2].

The study explained that the thermal imager's ability to be turned on before wetting the tablets and its non-contact nature allow for capturing the disintegration process from the beginning. This existing technique for studying RDT disintegration is advantageous because it works with whole tablets in any simple container, such as a watch glass, petri dish, or beaker. The setup was fast, easy, and convenient for taking temperature readings and thermometric analysis [2].

Their research further investigated the possibility of correlating temperature changes within the tablets with disintegration patterns predicted by existing (subtraction method) and new methods. In other words, the study aimed to establish a thermometry-based method for analyzing RDT profiles and disintegration. Fexofenadine hydrochloride (FEX HCl), a water-soluble, non-drowsy antihistamine medication, was chosen as a model drug. This drug is commercially available as the RDT brand Allegra™ [2]. Their study acknowledged that alternative, high-end techniques might offer better temporal resolution for analyzing RDT disintegration. However, the authors emphasized the advantages of thermal imaging: it's very cost-effective, portable, and user-friendly for studying FEX RDT disintegration. The passage also mentioned that advancements in imaging technology and high-speed thermal cameras could potentially capture disintegration in fractions of a second in the future [2].

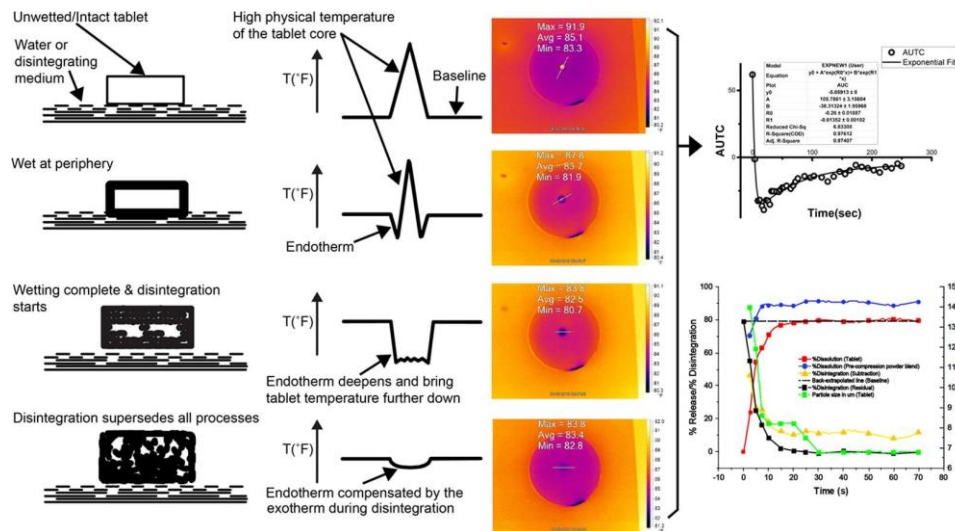


Figure 1. Represents the thermal imaging technique for disintegration screening [2]

## 2.2. Modelling the Evolution of Pore Structure during the Disintegration of Pharmaceutical Tablets [3]:

### 2.2.1. Liquid Penetration and Tablet Swelling [3]:

The study by Daniel Markl et al. investigated liquid penetration and tablet swelling using a custom flow cell and a commercial terahertz pulsed imaging system (TPI) from Teraview Ltd. (Cambridge, UK). The specific model used was the TeraPulse 4000. For the TPI setup, a fiber-based reflection probe with an 18 mm silicon lens was employed to focus the terahertz beam. The probe head was designed to allow for easy spatial adjustments through linear scaling. The THz optics produced a beam with a waist of about 1 mm at the focus point, with an incident angle of 13 degrees. The authors noted that the TPI setup with the flow cell measured the change in the tablet's back face, which reflects the swelling of both the front and back faces due to liquid uptake (Figure 2a). It was further mentioned that the DEM simulation (Figure 2b) only captured the front face swelling because the flow cell was not included in the modeling process

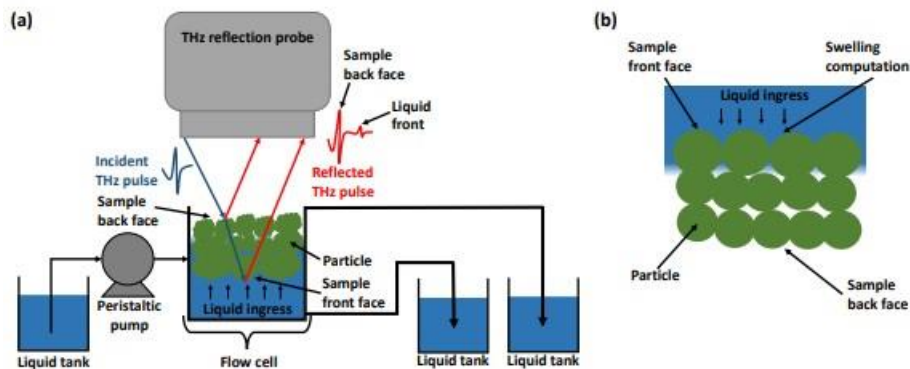


Figure 2. A schematic of the (a) experimental and (b) DEM modelling domain [3]

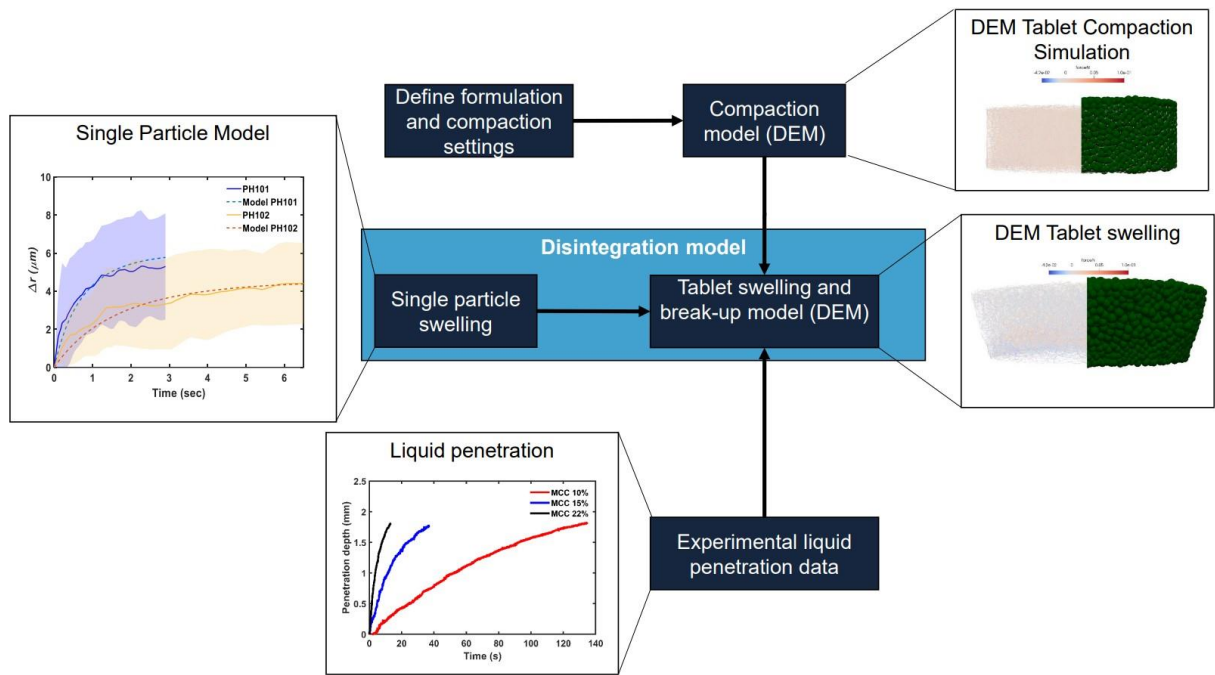
### 2.2.2. Modelling:

The integration of the models and experimental data to mimic tablet swelling and break-up is summarized in the figure shown in Figure 3. The model consisted of three main parts:

1. Experimental data on how liquid penetration the tablet.
2. A DEM (Discrete Element Modeling) tablet compaction model.
3. A DEM disintegration model that incorporated a single-particle swelling model.

The study also mentioned Yade-DEM, an open-source DEM program, which offers both compaction and disintegration models.

Figure 3. Work flow of the tablet swelling and break-up model. A single-particle model, DEM tablet compaction model, and experimental liquid penetration data are combined to model the swelling and break-up process.[3]



**2.2.3. Tablet Compaction:**

Their study described the simulation process for mimicking the compaction of tablets. To represent the loose packing of particles under gravity, spherical particles were virtually compressed within a cylindrical compression die with a height of 3 mm and a radius of 1 mm. In order to reduce computational costs, the simulated tablet was shrunk to a diameter of 2 mm and a thickness of 0.8–1 mm while maintaining the experimental particle size distribution within the DEM simulation.

Then mentioned that the Luding elastoplastic contact model [7] was used to simulate interactions between particles (particle-particle) and between particles and the walls (particle-wall). Equations (1) – (3) were not explicitly provided but referenced as defining the normal force (Fn) within this model.

$$F_n = \begin{cases} k_1 \delta_n & \text{if } k_2(\delta_n - \delta_0) > k_1 \delta_n \\ k_2(\delta_n - \delta_0) & \text{if } k_1 \delta_n > k_2(\delta_n - \delta_0) \\ -k_c \delta_n & \text{if } -k_c \delta_n > k_2(\delta_n - \delta_0) \end{cases}$$

where  $\delta_n$  denotes the normal overlap,  $\delta_0$  the plastic contact deformation overlap,  $k_c$  the adhesion stiffness,  $k_1$  the loading stiffness, and  $k_2$  the plastic unloading stiffness. The technical term of  $k_2$  is:

$$k_2 = \begin{cases} k_p & \text{if } \frac{\delta_{max}}{\delta_{lim}} > 1 \\ k \frac{(k_p - k_1)\delta_{max}}{1 + \frac{\delta_{max}}{\delta_{lim}}} & \text{if } \frac{\delta_{max}}{\delta_{lim}} < 1 \end{cases} \tag{2}$$

where  $k_p$  is the maximum stiffness of plastic unloading. The plastic limit and the maximum compression overlap are represented by  $\delta_{lim}$  and  $\delta_{max}$ , respectively (see Equation (3)).

$$\delta_{lim} = \frac{k_p}{k_p - k_1} \phi_f R^* \tag{3}$$

where  $R^*$  is an analogous radius and  $\phi_f$  is the dimensionless plasticity depth. According to reference [8], the Luding elasto-plastic model's parameters  $k_1$  (loading stiffness) and  $k_p$  (limit plastic unloading stiffness) as well as the particle density primarily influenced the compression profile. By adjusting these three parameters, the majority of the compression profile's variations could be accommodated. By calibrating the particle density, [8] adjusted the model to account for the increased particle size in comparison to the tests. Because the model's particle size in this work matched that of the experiments, the observed particle's (actual) density was utilized for the simulations.

Through an optimization process that minimizes the error between the porosity values computed from the DEM model and the experimental data, the two unknown parameters in the model,  $k_1$  and  $k_p$ , were found. This was carried out for the pure MCC tablets at a medium compression pressure (15% porosity tablets), and the results from the low- and high-compression pressure trials were used to validate it. The calibration technique was developed using the research work. Since  $k_1$  only has an impact on the loading stage of the compaction process, many values of  $k_1$ , from 500 to 20,000 N/m, were simultaneously simulated using Yade's batch simulation mode.

To determine the ideal value, the root mean squared error (RMSE) between the simulated tablet porosity and the experimental tablet porosity under loading for different  $k_1$  values was minimized. Reference [9] emphasized that the deviation of the actual particle is the main factor causing the difference between the original experimental porosity and that of a simulated DEM tablet from the DEM's presumed spherical shape. The DEM does not take into account additional elements like surface asperities and intra-particle porosity that might have an impact on the powder's initial packing. There was an inaccuracy in the estimation of  $k_1$  due to this initial porosity difference. The porosity in the loading process was adjusted to a value between 0 (lowest observed porosity) and 1 (highest observed porosity) in order to minimize the impact of this initial variation in the packing of the powder. The ideal  $k_1$  value was then determined using the estimated RMSE values.

### 2.2.3. Disintegration Model:

The authors explained how they ensured the stability of the simulation by setting a time step of  $\Delta t = 10^{-6}$  s/step. They then described a single-particle swelling model, originally introduced by Reference [10], which was used to update the mass, inertia, and radius of each individual particle written in equation (4)-(12) and also swelling mechanism of the SAPs (super absorbent polymer). This model aimed to simulate the swelling mechanism. The underlying concept, according to the study, is that the difference in a particle's chemical potential compared to the surrounding liquid (water) drives the particle's expansion [11]. The specific equations for this single-particle swelling model were not explicitly provided in the passage.

$$\frac{dr_{p,i}}{dt} = f_w \frac{D_{qs}}{r_{p,i} \rho_w} \left( \frac{Q_i^{max} - Q_i^{abs}}{Q_i^{abs}} \right) \quad (4)$$

$$Q_i^{abs} = \left( \frac{m_i^w + m_i^s}{m_i^s} \right) = \frac{r_{p,i}^3 \rho_w}{r_{p,0}^3 \rho_w} - \frac{\rho_w}{\rho_s} + 1 \quad (5)$$

where  $r_p$  is the particle radius at time  $t$ , and  $r_{p,0}$  is the starting particle radius.  $\rho_w$  is the density of the liquid (in this case, deionized water), and  $\rho_s$  is the density of a dry particle. Assuming a constant diffusion coefficient,  $D$  ( $\mu\text{m}^2/\text{s}$ ) represents the water molecule's diffusion within the particle. The highest absorption ratio is known as  $Q_{max}$ .

This approach is not applicable when the particle is a component of a little tablet as it assumes that the particle is completely submerged in the liquid. Particles in a tiny tablet establish connections with one another over a contact area. As a result, the particle's effective, or accessible, surface area exposed to the absorbing liquid is decreased. This is explained by adding the component  $f_w$  to Equation (4), which expresses the ratio of the total particle surface area ( $A_p = 4\pi r_p^2$ ) to the accessible surface area ( $A_{actual}$ ).

$$f_w = \frac{A_{actual}}{A_p} \quad (6)$$

The particle surface area, or  $A_{actual}$ , is equal to the total of the areas that overlap with adjacent particles.

(7)

$$A_{actual} = A_p - \sum_i^n A_{cap,i}$$

$A_{cap}$  is defined as a function of the particle, centroid  $i$ ,  $x_i, y_i, z_i$ , and the coordinate of the contact point between particles  $i$  and  $j$  ( $x_j, y_j, z_j$ ). It is the surface area of the normal displacement volume between two neighboring particles, particles  $i$  and  $j$ . The number of nearby particles is represented by  $n$ .  $A_{cap}$  is provided as

$$(8)$$

$$A_{cap} = 2\pi r_p h$$

Using  $h$  as the overlapping cap's height, which is defined as

$$h = r_p - \sqrt{(x_j - x_i)^2 + (y_j - y_i)^2 + (z_j - z_i)^2} \quad (9)$$

Using the experimental data, the liquid's location was additionally updated every 100,000th time step. The liquid front position in the tablet at the simulation time points could be calculated due to the fitting of a power law ( $y = a \cdot t^b$ ) to the experimental results, The model takes the available wetted surface area to be  $A_{actual}$ . The simulation of a single-particle swelling assumes that a particle begins to inflate once the liquid reaches the particle center. In order to incorporate the particle size change into the DEM, a growth factor ( $f$ ) was defined.

$$f = \frac{r_p(t + M\Delta t)}{r_p(t)} = 1 + \frac{M\Delta t}{r_p(t)} \frac{dr_p}{dt} \quad (10)$$

The particle mass, inertia, and radius were only changed every 100,000th time step ( $M = 100,000$ ) in order to speed up the simulation. The radius at time  $t + M\Delta t$  is given by  $r_p(t + M\Delta t)$ . The mass ( $m$ ) and inertia ( $J$ ) of a particle were also changed as a result of the particle absorbing the liquid:

$$m(t + M\Delta t) = m(t) \cdot f^3 \quad (11)$$

$$J(t + M\Delta t) = J(t) \cdot f^5 \quad (12)$$

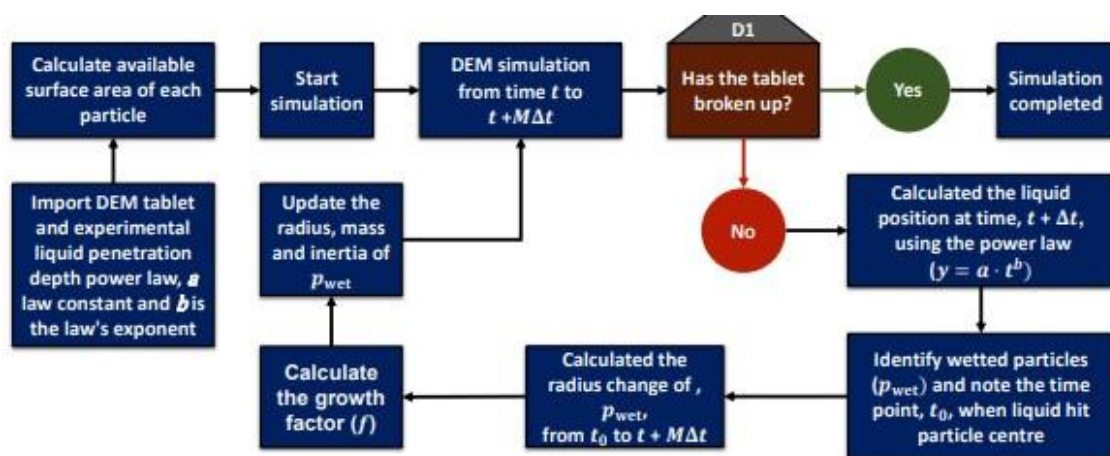


Figure 4. shows the whole process for simulating tablet swelling and breakage.[3]

### 2.2.4. Pore Structure Analysis of DEM Results:

From authors study voxel porosity technique [12] was used to measure the porosity. Using this method, the entire volume is divided into a dense grid of voxels at a certain resolution (200 μm), and all voxels that lie inside any particle are counted. Porosity, or  $e$ , is computed as

$$\epsilon = \frac{V - V_v}{V} \quad (13)$$

where  $V_v$  is the volume of voxels that lie inside any particles and  $V$  is the tablet's volume.

The triangulation and pore finite volume approach outlined in [13] and later [10] were used to calculate the pore diameters. Initially, solid particle centers were used as the vertices of the tetrahedra in a triangulation process applied to the tablet's pore space. The pore space is defined by the tetrahedron, which extends over four nearby particles. This is known as a pore unit. The radius of the tetrahedron's inscribed circle was then used to compute the size of each pore unit in the tablet.

Maps of cumulative porosity were created in order to analyze the pore space geographically. The details of this procedure are provided in reference [14]. In summary, a 3D vector representation of the tablet was created using PoreSpy [15] by using the location and radius of the particles. For this research, a cuboid portion ( $1400 \times 1400 \times 800 \mu\text{m}^3$ ) of the tablet's center voxel image was chosen. The maps were produced by dividing the total number of voxels for each dimension (x, y, and z) by the sum of the voxels categorized as voids along each axis. The void % is shown on the produced maps at each place.

### 3. Conclusion:

In this review, we have given the new techniques for tablet disintegration screening that may provide accurate evaluation data of tablet disintegration. The technique of thermal imaging will capture the thermometry during the disintegration of the tablet. By interpreting the thermal change to the amount, we can predict the disintegration rate with mass over time by knowing the specific heat capacity (the amount of energy required to raise the temperature of the unit mass by one degree) of the component and you can measure its temperature change over time, you might be able to estimate its mass based on the heat transfer observed in the thermal image. And coming to the modeling evaluation of the pore structure of the tablet disintegration, we can simulate the pore structural analysis and its influence on the tablet disintegration.

### 4. Acknowledgement:

The authors thank to the Jasbir Singh and et al. Post-Graduate Institute of Pharmaceutical Science (formerly college of Pharmacy), University of Health Sciences, Rohtak and Daniel Mark and et al. Strathclyde Institute of Pharmacy and Biomedical Sciences, University of Strathclyde, Glasgow G4ORE, UK for their research publications.

5. Conflict of interest statement: The authors report no conflicts of interest. The authors alone are responsible for the content and writing of this article.

### 6. REFERENCES:

1. Sravani S, Sailaja P. Formulation and Evaluation of Fast Dissolving Tablets of Felodipine. *IOSR Journal of Pharmacy*. 2016;6(7):104-12.
2. Ruhil S, Dahiya M, Kaur H, Singh J. New insights into the disintegration mechanism and disintegration profiling of rapidly disintegrating tablets (RDTs) by thermal imaging. *International Journal of Pharmaceutics*. 2022 Jan 5;611:121283.
3. Soundaranathan M, Al-Sharabi M, Sweijen T, Bawuah P, Zeitler JA, Hassanizadeh SM, Pitt K, Johnston BF, Markl D. Modelling the evolution of pore structure during the disintegration of pharmaceutical tablets. *Pharmaceutics*. 2023 Feb;15(2):489.
4. Braile D, Hare C, Wu CY. DEM analysis of swelling behaviour in granular media. *Advanced Powder Technology*. 2022 Nov 1;33(11):103806.
5. Soundaranathan M, Vivattanaseth P, Walsh E, Pitt K, Johnston B, Markl D. Quantification of swelling characteristics of pharmaceutical particles. *International journal of pharmaceutics*. 2020 Nov 30;590:119903.
6. Šmilauer V. *Yade Documentation 3rd ed. The Yade Project*.
7. Luding S. Introduction to discrete element methods: basic of contact force models and how to perform the micro-macro transition to continuum theory. *European journal of environmental and civil engineering*. 2008 Aug 1;12(7-8):785-826.
8. Gao Y, De Simone G, Koorapaty M. Calibration and verification of DEM parameters for the quantitative simulation of pharmaceutical powder compression process. *Powder technology*. 2021 Jan 22;378:160-71.
9. Thakur SC, Ahmadian H, Sun J, Ooi JY. An experimental and numerical study of packing, compression, and caking behaviour of detergent powders. *Particuology*. 2014 Feb 1;12:2-12.
10. Sweijen T, Chareyre B, Hassanizadeh SM, Karadimitriou NK. Grain-scale modelling of swelling granular materials; application to super absorbent polymers. *Powder technology*. 2017 Aug 1;318:411-22.
11. Huyghe JM, Janssen J. Quadriphasic mechanics of swelling incompressible porous media. *International Journal of Engineering Science*. 1997 Jun 1;35(8):793-802.
12. Markl D, Zeitler JA. A review of disintegration mechanisms and measurement techniques. *Pharmaceutical research*. 2017 May;34(5):890-917.
13. Chareyre B, Cortis A, Catalano E, Barthélemy E. Pore-scale modeling of viscous flow and induced forces in dense sphere packings. *Transport in porous media*. 2012 Sep;94:595-615.

- 
14. Markl D, Strobel A, Schlossnikl R, Bøtker J, Bawuah P, Ridgway C, Rantanen J, Rades T, Gane P, Peiponen KE, Zeitler JA. Characterisation of pore structures of pharmaceutical tablets: A review. *International journal of pharmaceutics*. 2018 Mar 1;538(1-2):188-214.
  15. Gostick JT, Khan ZA, Tranter TG, Kok MD, Agnaou M, Sadeghi M, Jervis R. PoreSpy: A python toolkit for quantitative analysis of porous media images. *Journal of Open-Source Software*. 2019 May 1;4(37):1296.